ELSEVIER

International Journal of Mass Spectrometry 176 (1998) 237–244

International Journal of Mass Spectrometry

Laser induced vaporization mass spectrometric studies on Si_3N_4

M. Joseph, N. Sivakumar, P. Manoravi

Materials Chemistry Division, Indira Gandhi Centre for Atomic Research, Kalpakkam 603 102, Tamil Nadu, India

Received 11 September 1997; accepted 23 March 1998

Abstract

An Si_3N_4 sample was irradiated with an Nd-YAG laser. The species present in the plume were detected by a quadrupole mass spectrometer (QMS). The species observed were Si, SiN, Si_2, Si_2N, Si_3, Si_3N, Si_4, Si_3N_4, Si_6, Si_7, and N. Weak signals were observed at $m/e = 126$ and 280. The analysis of the velocity of the different species indicates the existence of thermal equilibrium in the vaporization process. (Int J Mass Spectrom 176 (1998) 237–244) © 1998 Elsevier Science B.V.

Keywords: Laser vaporization; Time resolved mass spectrometry; Si_3N_4

1. Introduction

Silicon nitride (Si_3N_4) is used in a variety of applications such as high performance engineering components [1], semiconductor devices [2], and so forth. Currently, there is considerable interest in gaseous silicon nitrides, SiN [3], Si_2N [3, 4], Si_3N [3, 5], and SiN_2 [6], in order to understand the nature of bonding and other properties of these species. These studies are expected to provide the necessary information required for the formation of silicon nitride films for semiconductor devices [2,7].

Recently, laser ablation of thin films of Si_3N_4 was reported by two groups [8,9]. Takigawa and Hemminger [8] used an ArF excimer laser ($\approx 3 \times 10^9$ W/cm^2) to ablate the Si_3N_4 films and a Fourier transform mass spectrometer was used to identify the ionic species. Only two peaks were observed at 28 and 70 u and these were attributed to Si^+ and $(Si_3N_4)^{2+}$. Later Wang et al. [9] carried out similar studies on thin films, as well as on Si_3N_4 powder. They used the 266-nm beam of an Nd-YAG laser at a power density of $\approx 2 \times 10^7$ W/cm^2, to ablate the sample and the 355 nm beam from another Nd-YAG for ionization. A reflectron time-of-flight mass spectrometer was used to identify the vapor species. They also observed two intense peaks at 28 u and 70 u. These two peaks were unambiguously assigned to Si^+ and Si_2N^+. [But in earlier studies [8], peak at m/e of 70 was assigned to $(Si_3N_4)^{2+}$.] They also observed less intense signals at m/e of 42 and 56. These two peaks were assigned to SiN^+ and Si_2^+. More recently, Rocabois et al. [10] studied thermal evaporation of Si_3N_4 using a Knudsen cell and observed seven vapor species, namely, N, N_2, Si, SiN, Si_2, Si_2N, and Si_3. The present study is an attempt to study the very high temperature vaporization behavior of Si_3N_4 by using a laser induced vaporization mass spectrometric (LIV-MS) method [11]. The results obtained are reported here.

* Corresponding author.

PII S1387-3806(98)14016-2

2. Experimental

The details of the experimental facility are given elsewhere [12]. Briefly, this facility contains two chambers. The first chamber (target chamber) is pumped to a base pressure of $\approx 10^{-7}$ Torr by a diffusion pump (2000 L/s, M/s Edward's, UK). The second chamber is pumped by a cryopump (1500 L/s, M/s Leybold) to a base pressure of $\approx 10^{-8}$ Torr. A quadrupole mass spectrometer (QMS) (M/s Extrel, Model C50) is housed in this chamber in a crossed beam configuration. A *Q*-switched Nd-YAG laser (M/s Continuum Model NY/61) operating at 532 nm, having a pulse width of 8 ns and an energy of about 40 mJ is used as the heat source. This beam ($\approx$6 mm diameter) is focused on the sample, by using a quartz lens. The laser power density is varied by adjusting the distance between the focusing lens to target. The target is mounted on a remotely controlled micropositioner, and the target movement minimizes cratering effects. For the experiments reported here, the target material has been rastered at a speed such that $\approx$90% shot-to-shot overlap occurs on the focused laser spot. The ions that are formed in the vaporization process are deflected away from the beam axis using deflection plates. The neutral species reach the ionizer of the QMS and get ionized. Signal from the secondary electron multiplier detector, after amplification, is fed to a digital storage oscilloscope (DSO). In order to get a good signal-to-noise ratio, the signal is averaged in the scope for 1000 laser shots and stored. Generally, the collection of the signal for about 5 ms from the start of the laser pulse is found to be sufficient to get a time-of-arrival (TOA) profile. The data collected are transferred to the computer for further processing. By tuning the QMS for different masses of interest, the intensity and velocity distribution of each species formed in the laser vaporization can be obtained from the TOA profile.

The Si_3N_4 sample is obtained from M/s Cerac in the form of granules and has a purity of ~98%. The supplier's analysis as well as our XRD examination reveal the presence of α,β phases of Si_3N_4 and trace levels of Si_2ON_2. This sample was powdered and pellets (12 mm in diameter and 5 mm in diameter) were made out of it by cold pressing at 8 MPa, followed by sintering at 1500°C in flowing N_2 for about 12 h. This was not sufficient and the pellets so obtained were found to have only $\approx$70% of the theoretical density and were used in the laser induced vaporization study. An effective sintering method for Si_3N_4 has not yet been identified.

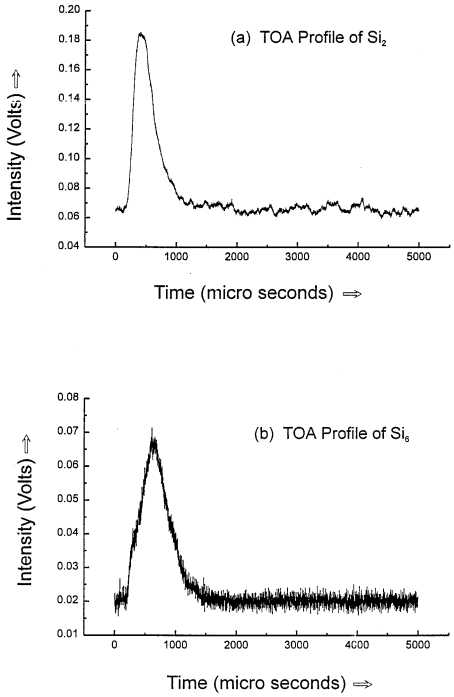

Fig. 1. Time-of-arrival spectra of Si_2 and Si_6 vapor species generated at a power density of 1×10^8 W/cm^2.

3. Results and discussion

The Si_3N_4 pellet is vaporized at two power densities, namely at 3×10^7 and 1×10^8 W/cm^2. At higher power densities ($>1 \times 10^8$ W/cm^2), large amounts of ions are produced that could not be deflected completely by the deflection plates. By tuning the QMS for different masses of interest, the TOA profile of each species present in the vapor is obtained. For example, the TOA spectrum obtained for the species Si_2 and Si_6 are shown in Fig. 1. From the TOA profile, the intensity of each species can be obtained. The

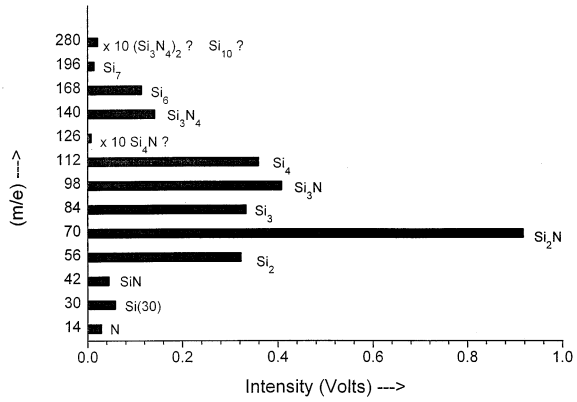

Fig. 2. Mass spectrum of vapor species formed from Si_3N_4 pellet at a power density of 1×10^8 W/cm^2. All the species were detected by using 30 eV ionization energy.

signal obtained at various m/e values, at power density of 1×10^8 W/cm^2 and ionization energy of 30 eV, is shown as a mass spectrum in Fig. 2. Except for Si, the most intense isotopic peak of the respective species are shown. For Si, the intensity of isotope 30 is shown. The signal observed at *m/e* of 14, 30, 42, 56, 70, 84, 98, and 112 was assigned to N, Si, SiN, Si_2, Si_2N, Si_3, Si_3N, and Si_4, on the basis of earlier studies [4,5,10] and from the isotopic ratios. The signal at 56 u is assigned to Si_2 on the basis of the isotopic ratio. Even though SiN_2 has been observed by reaction of Si atoms in N_2 matrix [6], no mass spectrometric observation has been reported. The contribution from this species to the signal at mass 56 may be very small and it is difficult to confirm from the isotopes ratio (Table 1). In earlier vaporization (both in laser and thermal) studies on Si_3N_4, no species has been observed beyond mass Si_3. But in this study, we have observed clear signal at *m/e* values of 140, 168, 196, and 280. However, the peak at $m/e = 126$ was seen only at the higher power density (1×10^8 W/cm^2). For each of these high mass peaks, different species can be assigned. For example, for the peak at 140, 168, and 196, the possible species that can be assigned are indicated in Table 1. The possible isotopic ratios expected are also shown in Table 1 along with the observed values. From these data, the peaks observed at these three *m/e* values, namely, 140, 168, and 196, can be assigned to Si_3N_4, Si_6, and Si_7 respectively. The peaks obtained at *m/e* of 126 and 280 are very weak and no definite isotopic ratios could be obtained. But tentatively the peak at 126 u is assigned to Si_4N. The peak at 280 can be due to Si_{10} or the dimer of Si_3N_4 or any other suitable combination of Si and N atoms. For a power density of 3×10^7 W/cm^2, the observed intensities, as well as the intensities after correction for isotopic abundance, ionization cross section [13], and ion transmission coefficient [14], are shown in Table 2.

The main objective of this study was to measure the partial pressures of various species at very high temperatures (>3000 K) by using the LIV-MS method [11]. In this method, one has to establish that the vaporization is a thermal process and be able to assign a definite surface temperature. Then, the intensities of various species can be used to determine the partial pressures.

As early as 1965, Ready [15] considered pulsed laser absorption by solids and the consequent transient temperature rise. He pointed out that even for *Q*-switched laser pulses the temperature is defined, although they may even be above the critical temperature. This is because the transfer of energy from the excited electrons to the lattice is very fast; of the order of 10^{-13} s, so that it can be regarded that the energy absorbed from the laser radiation instantaneously

Table 1
Intensity ratios (expected and observed) for various possible species at $m/e = 56$, 140, 168, and 196

	$m/e = 56$			$m/e = 140$			$m/e = 168$				$m/e = 196$			
Intensity ratio	Si_2	SiN_2	Obs.	Si_5	Si_3N_4	Obs.	Si_4N_4	Si_3N_6	Si_6	Obs.	Si_5N_4	Si_4N_6	Si_7	Obs.
$m/(m+1)$	9.8	19.7	10.5	3.9	6.5	5.8	4.9	6.57	3.29	3.4	3.95	4.9	2.82	2.6
$m/(m+2)$	14.3	29.7	16	5.1	9.2	9.7	6.7	9.2	4.17	4.02	5.16	6.7	3.46	3.3

Key: obs., observed.

Table 2
Intensity and Botlzmann fitted velocities and temperatures for the various species formed over Si_3N_4

Species	Observed intensity (V)	Observed area (au)	Correction factor	τ_i	σ_i	Corrected intensity (V)	Corrected area (au)	Velocity v_{g1} (cm/s)	Velocity v_{g2} (cm/s)	Temperature T_1 (K)	Temperature T_2 (K)
Si	0.0958	38.7	32.2	1	5.286	0.58	235.74	0	200,000	600	3000
SiN	0.026	20.27	1.09	1	6.4824	4.37×10^{3}	3.41	0	140,000	3000	3000
Si_2	0.2664	111.8	1.176	1.1	10.572	2.69×10^{-2}	11.30	0	140,000	2000	3000
Si_2N	0.518	385.6	1.176	1.2	11.7684	4.31×10^{-2}	32.11	0	150,000	600	3000
Si_3	0.168	65.78	1.274	1.1	15.858	0.012	4.80	0	130,000	1500	3000
Si_3N	0.0045	2.53	1.274	0.9	17.054	3.73×10^{-4}	0.21	0	100,000	1500	3000
Si_4	0.128	58.66	1.38	0.9	21.144	9.28×10^{-3}	4.25	0	105,000	1500	3000
Si_3N_4	0.0504	22.6	1.274	0.8	20.6436	3.88×10^{-3}	1.74	0	100,000	1500	3000
Si_6	0.0598	26.97	1.6247	0.6	31.716	5.10×10^{-3}	2.30	0	90,000	1000	3000
Si_7	0.0049	3.09	1.7615	0.5	37.002	4.66×10^{-4}	0.294	0	80,000	1000	3000
$(Si_3N_4)_2$	0.0013	0	1.6247	0.3	41.2872	1.70×10^{-4}	0.294	0	65,000	500	3000
N[a]	0.03	36	1	0.7	1.1964	3.58×10^{-2}	42.98	0	≈100,000	1000	3000

The arrival time profiles and velocity distributions for molecules produced by laser vaporization are discussed in [31]; our profiles fit with two distributions and these are interpreted as arising from (1) molecule vaporizing from the surface at temperatures near the peak surface temperature (collisional expansion giving rise to a group velocity because of large densities) and (2) an effusive (group velocity equal to 0) component arising from molecules vaporizing at intermediate temperatures (low densities) present on the falling side of the temperature vs. time curve [21].

[a]Because of large background from N_2 present at the base pressure of the chamber, could not be fitted clearly.

Key: τ_i, transmission coefficient; σ_i, ionization cross-section at 30 eV; the definitions of the parameters are given on p. 241.

becomes thermal energy in that volume. Many groups have studied vapor pressures of refractory materials by coupling laser vaporization with mass spectrometry. A good number of them have used millisecond pulsewidth lasers; e.g. Olander et al. [16]; Ohse et al. [17] have used microsecond pulsewidth lasers; and Hastie et al. [18] have used nanosecond pulsewidth lasers.

The question often raised is whether there is thermal equilibrium for heating with nanosecond pulsewidth lasers. There is no solid–gas equilibrium in the sense that there is for knudsen cell studies, where the effusion rate from gas in equilibrium with the solid is measured. For free vaporization in vacuum, we measure a vaporization rate and as long as there is a defined surface temperature, the vaporization rate is defined and will be equal to the equilibrium condensation rate of the gas in equilibrium with the solid. The energy of the vapor molecules, in their respective degrees of freedom, will also be given by this temperature; for instance, see the study of laser vaporization of graphite by using nanosecond laser pulses by laser induced fluorescence spectroscopy of C_2 performed close to the surface [19].

We measured in our experiments a linear dependence (other than for small deviations for large masses due to a spatial separation of masses in the collision region of the expansion) of the group velocity on the inverse of the square root of the mass of the molecule for all the systems that we have studied. This indicates a common thermal source, because the collisions in the subsequent supersonic expansion, if anything, will only obscure this dependence. Our surface temperature estimates were made from this dependence. Furthermore, reassuringly, we found that for temperatures for which the vaporization rates are such that there is effusion, the velocity distributions are better fit as an effusive source with a definite temperature without the inclusion of any group velocity. We also found that it is possible to change this surface temperature by varying the power density incident on the surface.

For high enough temperatures (depending on the system studied) the ion and electron densities are

large and the vapor is indeed a plasma. The densities of the ions, electrons, and neutral particles at the surface are related by the Saha equation [20]:

$$\left(\frac{n_e n_p}{n_a}\right) = \left(\frac{2\pi m_e kT}{h^2}\right)^{3/2} \exp\left(\frac{-I_{\text{eff}}}{kT}\right)$$

where n_e, n_p, n_a are the electron, ion, and neutral densities, respectively, T is the surface temperature, and I_{eff} is the effective ionization potential for the molecule at the surface. Off the surface in the vapor they will be related by this expression with I, the ionization potential of the molecule in the gas phase replacing the I_{eff}. We do observe for all the systems that we have studied, an increase in the ions' signal intensity (measured with the ionizer of the ion source turned off) with an increase in the incident power density and therefore in the surface temperature. Further from the velocity of the ions, we have inferred that there is inverse Bremsstrahlung absorption of the laser radiation by the ions in the vapor [21].

For irradiation with nanosecond pulses there are thermal processes that occur as seen from the solidification of liquid silicon on the sides of the crater [22]. For irradiation with femtosecond pulses a clean crater is observed, suggesting that this is a photochemical process possibly due to multiphoton absorption [22]. Our experiments on graphite also show solidification of liquid carbon on the sides of the crater [23].

The difficulty with the nanosecond pulsewidth laser heating so far has been that a direct measurement of the temperature has not been possible, because the high temperature transient is present for only times of the order of the pulsewidth of the laser and therefore, ≈100 ps analog time resolution is necessary. Some reports have become available that make a fast real time measurement of the transient high temperature pulse by measuring the intensity of the emission from the surface [24].

We conclude that the vaporization process for the wavelength and power density used is indeed thermal in nature and further point out that a photochemical component is present for irradiation with very short wavelengths [25].

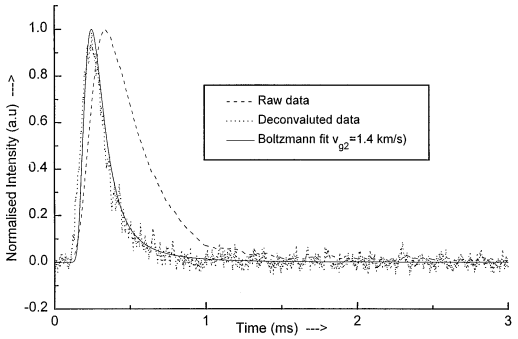

Fig. 3. Boltzmann fit for the time-of-arrival profile of Si_2. Flow velocity (Vg_2) is 1.4 km/s.

The surface temperature can be determined from the TOA profile [23]. The TOA profile obtained for each species was used to find the velocity by using a shifted Boltzmann fit, of the form [26],

$$f(t) = \Sigma_i A_i t^{-4} \exp\{-m[(z/t) - v_{gi}]^2/(2\ kT_i)\},$$

where $f(t)$ is the measured intensity at time t, A_i is a constant, m is the mass of the particle, z is the distance between the target and the detector, v_{gi} is the center-of-mass velocity, k is Boltzmann's constant, and T_i is the temperature describing the stream velocity spread. This fitting was done after deconvoluting the time constant of the detector electronics involved in the TOA measurement [21]. For example, the fitting done for Si_2 is shown in Fig. 3. The group velocity (v_g) and temperatures obtained for the various species are given in Table 2. The linear dependence of the flow velocity versus ($1/\sqrt{\text{mass}}$) as shown in Fig. 4 indicates that the vaporization is a thermal process and the estimated surface temperature from the slope is 4500 ± 300 K for the lower power density (3×10^7 W/cm^2). A similar procedure resulted in a surface temperature of 5000 ± 300 K for the higher power density (1×10^8 W/cm^2).

We now discuss the possibility that the clusters observed in these experiments arise because of condensation in the expansion and do not represent their vaporization rates from the surface. Clusters are formed by termolecular collisions (because a third body is necessary to carry away the condensation energy) in the expansion. The density in the expan-

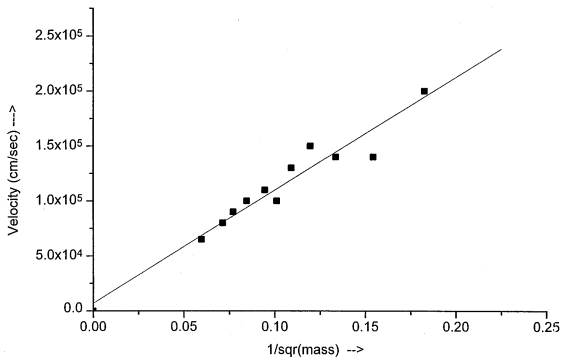

Fig. 4. Plot of velocity vs. $1/\sqrt{(\text{mass})}$ for various species that are observed over Si_3N_4 at a power density of 3×10^7 W/cm^2.

Table 3
Comparison of cluster intensities at two different temperatures (i.e. two different source pressures)

	Corrected intensities		
Species	4500 K	5000 K	Ratio
Si	0.58	0.95	1.64
Si_2	0.027	0.087	3.2
Si_3	0.0122	0.063	5.16
Si_4	0.0093	0.069	7.41
Si_6	0.0051	0.026	5.1
Si_7	0.0005	0.0037	7.4

$(P_0^2\ D)_{5000}/(P_0^2\ D)_{4500} = 1.65$.

sion falls as $(D/L)^2$, where D is the nozzle orifice diameter and L is the axial distance downstream. Therefore, the total number of termolecular collisions per molecule in the expansion is quite closely only those that occur in the volume that is within an axial distance of D from the nozzle orifice. The number of Si + Si + Si collisions per Si atom, for an Si partial pressure of 10 atm at 5000 K and an effective diameter σ of (2.5×10^{-8} cm) is given by

$$8\sqrt{2}\pi^2\sigma^5(n/v)^2c/\text{s}$$

where (n/v) is the number density and c is the speed. For the time that it takes these atoms to move across an axial distance, D, the total number of termolecular collisions per Si atom is ~20, and only a small fraction of these collisions are expected to be effective. It should also be noted that these collisions will be far less effective than the expansions using He, because He is a far more effective third body. In contrast is a study of alkali metals' dimers where the mole fraction of dimers (formed in the expansion) is found to be large [27].

Assuming that the Si_2 observed in our measurements is indeed caused by clustering in the expansion and assuming that none of the clusters' densities are saturated (as can be seen from Table 3) the ratio of the intensities of the clusters can be related (considering only the rate of formation using the same rate constant and not the equilibrium); e.g.

$$Si_2 + Si + Si \rightarrow Si_3 + Si$$

[(Si_3/Si_2) ratio would be the same as (Si_2/Si)]

$$Si_2 + Si_2 + Si \rightarrow Si_4 + Si$$

[(Si_4/Si_2) ratio should be the same as $(Si_2/Si)^2$]

$$Si_3 + Si + Si \rightarrow Si_4 + Si$$

[(Si_4/Si_3) ratio should be the same as (Si_2/Si)]

and so on. The successive observed ratios from the corrected intensities in Table 2 are a factor of 10 larger than those expected. We did not consider any collisions of four or higher because they would be negligible.

A comparison of the observed intensities (corrected for the difference in the focal area, i.e. D^2) at two different power densities is given in Table 3. The dimer-to-monomer ratio, under the assumptions that we have used to calculate the number of termolecular collisions in the expansion, goes as $P_0^2\ D$ [28], where P_0 is the source pressure. A $P_0\ D$ dependence is observed for conditions of large dimer densities [27]. In the coexpansion of OCS with He the small clusters are found to go (for the same D) as P_0^2 and then saturate, whereas the large clusters go as P_0^2 [29]. From Table 3 it is seen that even for Si_2, where the maximum dependence can be $(P_0^2\ D)$, the ratio is larger than that given by $P_0^2\ D$. The higher clusters have even larger ratios. It will be far more instructive to compare these ratios under conditions where source

pressures vary over an order of magnitude but we have available only these values.

We also point to the laser vaporization studies of graphite [18,23] and thermodynamic predictions [30] for the partial pressures of clusters of carbon atoms. For comparable or even larger pressures, the partial pressures of these clusters do not suggest any cluster formation in the expansion and are in qualitative agreement with thermodynamic calculations [30]. We conclude that although cluster formation in the subsequent expansion cannot be altogether discounted, the intensities observed for clusters in our experiments on Si_3N_4 primarily represent their vaporization rates from the surface at the estimated temperatures.

To perform partial pressure measurements, the signal obtained for each pulse should be stable and truly reflect the vaporization rates for that temperature. Generally, in this type of laser vaporization experiment the signal will not be steady because of crater formation and the change in the reflectivity of the surface on irradiation. In the latter case, the change in reflectivity reduces the absorbed energy and therefore the temperature; so that the reduced signal intensity does truly represent the intensity that should be observed at that temperature. In the case of crater formation the surface temperature may be the same but the observed intensity is less because of crater effects: e.g. condensation on the crater walls. The effect of crater formation can be minimized by rastering the sample during the laser irradiation. Generally, 90% shot-to-shot overlap of the irradiated spot is found to be sufficient to have a steady signal [11]. However for the present experiment, such rastering did not provide a steady signal. In Fig. 5 we compare the UO signal (on vaporization of UO_2) and Si_2N signal (on vaporization of Si_3N_4) at a surface temperature around 4500 K as a function of number of laser shots that the spot has been exposed to, showing clearly the drop in Si_2N signal. The crater depths for UO_2 and Si_3N_4 in the above cases, as a function of laser shots that the spot has been exposed to, are given in Table 4. Clearly the reduction in signal correlates with the crater depth.

This effect seems to be particularly severe for Si_3N_4 and in our experiments on graphite for similar

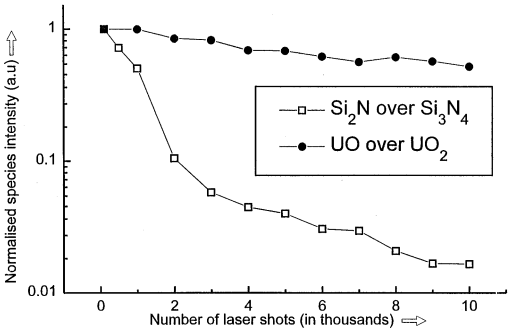

Fig. 5. Change in intensity of Si_2N species over Si_3N_4 and UO species over UO_2 pellet for different number of laser shots.

or even larger depths per laser shot we observed a steady signal on rastering [23]. The graphite disc used is commercially available (Leico Industries, Inc, USA) with the density guaranteed to be uniform and $>$90% of the theoretical value. The Si_3N_4 pellets used have only $\approx$70% of the theoretical density and the density may not be uniform because the sintering is ineffective, as seen from a comparison of the density before and after sintering. This may lead to an inhomogeneous temperature profile over the focal area and an uneven surface. We believe that using high and uniform density pellets will be advantageous for these experiments.

We also have to consider the system in terms of the number of phases and components present as the analysis reveals the presence of three phases in the sample (see Sec. 2). Neglecting the Si_2ON_2 phase that is present in trace levels, the vaporization is given by the equilibrium of two solid phases (α,β phases of Si_3N_4) with the gas phase, with each phase consisting of two components, Si and N. For this equilibrium the number of degrees of freedom is given by the phase

Table 4
Depth of crater measured for different number of laser shots on Si_3N_4 and UO_2 pellets for estimated surface temperature of about 4500 K

Pellet laser shots	Depth of crater (μm) for number of laser shots				
	100	500	1000	5000	10,000
Si_3N_4	10	17.5	25	30	35
UO_2	$<$0.1	—	0.2	—	0.5

rule and is equal to 1. Therefore, for any particular temperature there is a definite pressure, and it is independent of the composition. If the sample is a liquid at the measurement temperatures, then taking the liquid to be a single phase, the pressure at any given temperature is dependent on the composition as well. This is similar to knudsen cell measurements of constant intensity when a two component system of three phases (two solid phases and a gas phase) is in equilibrium, and after the phase transformation in the solid is complete, the measured intensity becomes a function of composition and eventually reaches the congruently vaporizing composition for that temperature [31].

Conclusions

We used an LIV-MS method to study the vapor phase composition present over Si_3N_4. We could detect 11 species, namely, Si, SiN, Si_2, Si_2N, Si_3, Si_3N, Si_4, Si_3N_4, Si_6, Si_7, and N. Very weak signals were also seen at m/e of 126 and 280. The peak at 126 is tentatively assigned to Si_4N. The vaporization process was found to be thermal in nature. Because of crater effects on the signal intensities, they cannot reliably be used for the determination of the true partial pressures, which can only be estimated.

References

[1] R.N. Katz, Science 208 (1980) 841.
[2] D.S.L. Mui, H. Liaw, A.L. Demirel, S. Strite, H. Morkoc, Appl. Phys. Lett. 59 (1991) 2847.
[3] N. Goldberg, M. Iraqui, H. Schwartz, A. Boldyrev, J. Simons, J. Chem. Phys. 101 (1994) 2981.
[4] R. Viswanathan, R.W. Schmude Jr. K.A. Gingerich, J. Chem. Thermodynam. 27 (1995) 1303.
[5] K.A. Gingerich, R. Viswanathan, R.W. Schmude Jr., J. Chem. Phys. 106 (1997) 6016.
[6] I.S. Ignatyer, H.F. Schaefer, III, J. Phys. Chem. 96 (1992) 7632.
[7] G.M. Nikolic, Vacuum 40 (1990) 143.
[8] Y. Takigawa, J.C. Hemminger, Appl. Surf. Sci. 79/80 (1994) 146.
[9] S.L. Wang, K.W.D. Ledingham, W.J. Jia, R.P. Singhal, Appl. Surf. Sci. 93 (1996) 205.
[10] P. Rocabois, C. Chatillon, C. Bernard, J. Am. Ceram. Soc. 79 (1996) 1351.
[11] J.W. Hastie, D.W. Bonnell, P.K. Schenck, High Temp. Sci. 25 (1988) 117.
[12] M. Joseph, N. Sivakumar, D.D.A. Raj, C.K. Mathews, Rapid Commun. Mass Spectrom. 10 (1996) 5.
[13] D.W. Bonnell, software SIGMA, version 1.1, NIST, Gaithersburg, MD, 1990.
[14] D.W. Bonnell, J.W. Hastie, in J.W. Hastie (Ed.), Characterization of High Temperature Vapors and Gases, Proceedings of the 10th Matl. Res Symp., NBS SP-561/1, US Government Printing Office, Washington, DC, 1979, p. 537.
[15] J.F. Ready, J. Appl. Phys. 36 (1965) 462.
[16] D.R. Olander, S.K. Yagnik, C.H. Tsai, J. Appl. Phys. 64 (1988) 2680.
[17] R.W. Ohse, J-F. Babelot, P.R. Kinsman, K.A. Lung, J. Magill, High Temp. High Press. 11 (1979) 225.
[18] J.W. Hastie, D.W. Bonnell, P.K. Schenck, High Temp. High Press. 20 (1988) 73.
[19] R.W. Dreyfus, R. Kelly, and R.F. Walkup, Nucl. Instrum. Methods Phys. Res. B 23 (1987) 557.
[20] R.W. Ohse, J.-F. Babelot, C. Cercignani, J.P. Heirnaut, M. Hoch, G.J. Hyland, J. Magill, J. Nucl. Mater. 130 (1985) 165.
[21] M. Joseph, N. Sivakumar, D.D.A. Raj, C.K. Mathews, J. Nucl. Mater. 247 (1997) 21.
[22] W. Katuek, J. Kruger, Mater. Sci. Forum 173–174 (1995) 17.
[23] M. Joseph, P. Manorvai, N. Sivakumar, C.K. Mathews, unpublished.
[24] D. Otte, H. Kleinschmidt, O. Bostanjoglo, Rev. Sci. Instrum. 68 (1997) 1.
[25] A. Costela, I. Garcia-Moreno, F. Florido, J.M. Figuera, R. Sastre, S.M. Hooker, J.S. Cashmore, C.E. Webb, J. Appl. Phys. 77 (1995) 2343.
[26] Q. Zhuang, K. Ishigoh, K. Tanaka, K. Kawano, R. Nakata, Japan J. Appl. Phys. 43 (1995) L248.
[27] R.J. Gordon, Y.T. Lee, D.R. Herschbach, J. Chem. Phys. 54 (1971) 2393.
[28] I.H. Levy, L. Wharton, R.Z. Smalley, in C.B. Moore (Ed.), Chemical and Biochemical Applications of Lasers, 2 (1977) 1.
[29] N. Sivakumar, Ph.D Thesis, Cornell University, (1986).
[30] H.R. Leider, O.H. Krikorian, D.A. Young, Carbon 11 (1973) 555.
[31] D.W. Bonnell, P.K. Schenck, J.W. Hastie, Ind. Symp. Laser Process for Microelectronic Applications, 172nd Electrochemical Society Meeting, 1987; J.W. Hastie, D.W. Bonnell, A.J. Paul, P.K. Schenck, Mater. Res. Soc. Symp. Proc. 285 (1993) 39.
[32] J.A. Roberts Jr., A.W. Searcy, Science 196 (1977) 525.